Visualization of Traffic Sign Related Rules Used in Road Environment-type Detection*

Z. Fazekas[1], G. Balázs[2], A. Boulmakoul[3], and P. Gáspár[1]
[1] Institute for Computer Science and Control (SZTAKI), Budapest, Hungary
[2] Zukunft Mobility GmbH, Kösching, Germany
[3] Computer Science Department, Faculty of Sciences and Technologies of Mohammedia, Hassan II Casablanca University, Morocco
e-mail: zoltan.fazekas@sztaki.hu, gabor.balazs@zf.com, azedine.boulmakoul@gmail.com, peter.gaspar@sztaki.hu

***Abstract*— A heuristic rule-based approach was proposed in a recent paper for the detection of the urban road environment-type (RET), such as downtown, residential area, and business/industrial area, that characterizes the road environment around an ego-car. The RET detection approach takes into account the relevant traffic signs (TSs) that are visible from the ego-car. It is assumed that the TS data, namely the type and the location of each detected TS along the route, is made available for the purpose by an on-board TS recognition system. The continually updated TS data is aggregated and evaluated in a multi-scale manner by the RET detection system. In the present paper, the heuristic rules – employed within the mentioned system – that handle the competition situations arising between the RET-candidates selected for and representing the various distance-scales are visualized in a vividly descriptive manner. The visualization of the rules makes the decision process easier to understand, furthermore, it facilitates the re-use, the adaptation and the extension of the rule-set for other road-related applications that rely on TS and possibly on other road-related data. A summary of the RET detection results from the mentioned paper is included herein to make the paper self-contained.**

I. Introduction

The sensing, computing and detection capabilities that have already been made available, and those that are expected to be made available in the near future on-board new production cars open fresh avenues in the development of smart driving solutions, and of additional functions and subsystems within advanced driver assistance systems (ADAS) [1]. A viable way toward such solutions, functions and subsystems is to put the gathered ADAS data – concerning the detected vehicles, lanes, road objects, and the ego-vehicle itself – to further use [2].

A traffic sign (TS) based urban road environment-type (RET) detection system was proposed in [3], which effectuate a supplemental driver assistance function along these lines; it relies on an existing ADAS subsystem, namely the TS recognition (TSR) subsystem, see e.g., [4]. The RET detection system gathers TS data along the route with the help of the TSR subsystem, and employs a stochastic change detection method in respect of the collected TS data to identify RET change-points.

* The work presented herein was supported by the National Research, Development and Innovation Office through the 2018-2.1.10-TÉT-MC-2018-00009 research contract.

Several variants of the aforementioned TS-based RET detection system were proposed later [5], [6], [7] and [8]. These rely on different computing techniques ranging from the shallow artificial neural networks (ANNs) – either modular [7], or non-modular [6] ones – to the heuristic rule-based decision making techniques [8]. Some of these systems, namely the ones presented in [5], [6], and [7], use additional input data, such as types and location of the encountered crossroads (CRs) along the route.

It should be noted that other types of input data (e.g., the number of dead-end roads, regularity of the street pattern, length of green/unbuilt sections) could be also considered for the given purpose. Such data could be gathered with a smart car equipped with a camera and LiDAR, but in most cases are available/derivable from geographical databases, as well.

Interestingly, the above types of data were among those used in [9] to assess the relationship between features of UK cities and certain socio-economic indicators, and in [10] to valorize street segments in the French Riviera.

In the studies presented in [5] to [8], three urban RETs were considered by the implemented systems. The road environment sweeping past the ego-car was classified into one of the following categories: downtown (Dt), residential (Res), and business/industrial areas (Ind).

II. Background

A. *RET Detection – An Important ADAS Function*

Initially, the authors of the present paper were not fully convinced whether the proposed ADAS function was of any practical significance, or not. Its usefulness had been, however, confirmed by a prior driving simulation study [11].

The effect of driving experience on drivers' adaptation to road environment complexity in urban areas was investigated in the cited study via monitoring drivers driving in a computer-simulated environment and via analyzing the driving data gathered.

Three levels of road environment complexity – matching roughly the aforementioned urban RETs – were used in the experiments. The drivers participating in the expe-

978-1-7281-5083-3/19/$31.00 ©2019 IEEE

riments were grouped into three groups according to their driving experience.

It turned out that the most experienced drivers displayed a greater degree of adaptation to increasingly complex urban road environments than the drivers in the other two groups. The authors of the cited paper opine that the driving experience results in an enhanced ability to appropriately assess the demands of the road environment.

For the drivers lacking prolonged driving experience, a RET detection ADAS function would be beneficial indeed. In the context of self-driving cars, the information on actual RET is also important; this information can be used in choosing appropriate speed and acceleration/deceleration.

B. *TS-based RET Detection*

In the TS-based RET detection systems brought up in the Introduction, the actual RET is inferred from the types and the along-the-route frequencies of certain TSs. The systems take into account only the relevant TSs that are visible from the ego-car, and use only an informative subset of TS-types for the decision making. The subset is shown in Fig. 1.

The TSs are grouped into three groups; the ones appearing within the group on the left are more typical to Dt areas, while the ones in the middle are more typical to the Ind areas, finally, the ones within the group on the right are more typical to the Res areas.

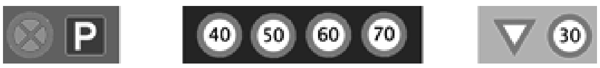

Figure 1. TSs used for the purpose of RET detection.

It is assumed that the TS data, namely the type and the location of each detected TS along the route, is made available for the purpose by an on-board TSR system.

C. *Car-based Data Collection Trips*

Several car-based data collection trips were carried out in respect of the TSs and urban RETs in three urban areas within Hungary. For these trips a tablet-based Android application was developed to facilitate manual data entry in respect of TSs and the RETs encountered along the route. The manual data logging was the task of a data entry assistant. The app geo-tags the data entries (e.g., the TS locations) and records the car-trajectory in an on-going manner. However, the recorded geo-coordinates are not used directly in the RET calculations, only the path-lengths between the recorded locations are used. For more details (e.g., maps, photos of typical road environments) on the data collection, see [3].

III. The Heuristic Rule-based RET-detection System

A heuristic rule-based approach was proposed in [8] for the detection of the urban RET from an ego-car. In this section, the main stages of the processing carried out by that system is summarized to make the present paper self-contained. In Section IV an intuitive graphic representation of the heuristic rules is introduced. It makes the competition handling procedure amongst the RET-candidates more understandable. The graphical representation employed herein facilitates the re-use, the adaptation and the extension of the rule-set for other road-related applications that rely on TS, and possibly on other road-related data.

A. *Multi-scale Evaluation of the TS-occurrences*

To explore the relationship between TSs and RETs along a route profusely, it is important to consider TS occurrences along different path-lengths measured backwards from the actual car-position. The motivations for this are as follows. The size of the road environments may vary. The distances between consecutive TSs may differ radically even within a given road environment, but also among different road environments. The selection of driving path can considerably affect how frequently TSs occur along the route [12]. By using TS data aggregated for several path-lengths, one can retain information that otherwise would be lost due to a single averaging effect.

For the above reasons, and to keep the number of scales low, three different path-lengths were selected for each of the TS-based RET detection systems mentioned in the Introduction. These path-lengths are the last 0.25 km, 0.5 km, and 1 km of the car-trajectory. The aggregations and evaluations over these trajectory-segments will be referred to as short (SR), medium (MR), and long-range (LR) aggregations/evaluations, respectively.

The continually updated TS data is aggregated and evaluated in a multi-scale manner by the heuristic rule-based RET detection system described in [8]. These heuristic rules handle the competition situations between RET candidates computed for the different distance-scales. The rules rely on categories (e.g., *Greatest*, *Loser*) borrowed from the sport-jargon, while these are derived and aggregated from the scores associated with the TS-occurrences over SR, MR and LR trajectory-segments.

B. *Individual and Aggregated Scores*

A procedure that estimates the influence of input signal values (e.g., the number of TS-occurrences that belong to the TS-types shown in the left group of Fig. 1) – along a given trajectory-segment – on the decision concerning RETs in a heuristic manner, and provides the basis for the comparison across different RETs was proposed in the above cited paper.

The scores associated with the TS-occurrences are aggregated (e.g., summed) for each RET over each of the distance-scales. After aggregation, Dt could score, say, 9, Ind 4, and Res -5 for SR, while Dt could score 5, Ind -1, and Res -7 for MR, and lastly, Dt 12, Ind -6, and Res 2 for LR. For details on how to choose the individual scores for the TS-occurrences and ways to aggregate the individual scores, see [8].

C. *Categories for Competition Handling – Borrowed from the Sport Jargon*

Categories are used for the purpose of characterizing and weighing the relationships based on the aggregated scores for each scale, and to facilitate the comparison of the 'competing' RET candidates. The labels of these categories were borrowed from the sport jargon: *Kicker:* the aggregated score for a given RET in a particular scale exceeds each of the other RETs' aggregated scores in the same scale at least by some predefined difference. *Greatest:* the aggregated score for a given RET in a particular scale exceeds each of the other RETs' aggregated scores in the same scale. *Second greatest:* the aggregated score for a given RET in a particular scale exceeds each but one of the other RETs' aggregated scores in the same scale. *Loser:* the aggregated score for a given RET in a particular scale is less than each of the other RETs' aggregated scores, respectively, in the same scale at least by some predefined difference.

For each scale, the aggregated scores are checked against these criteria. In each scale, each of the mentioned categories is associated with at most one RET at a particular road-location. This property is ensured, if necessary, by randomized selection between the possible RETs for the given category. For the sample scores given in the previous Subsection as an example, Dt would be *Kicker* and also *Greatest*, Ind would be the *Second greatest,* and Res would be a *Loser* for the purpose of RET selection at a particular road location.

D. Heuristic Decision Rules

Taking the categories determined for the different distance-scales (i.e., for SR, MR and LR), and their associations with the various RETs as input, sequential decision rules are used to determine the perceived RET. The following general order of the evaluation is adopted. It starts with the rules for the SR; these are evaluated firstly to ensure that the RET detection function reacts promptly to sudden changes; then, the rules concerning the LR categories are evaluated, which is followed by those concerning the MR categories. Furthermore, within each scale the rules concerning the *Kicker* and the *Loser* are evaluated before the ones concerning *Greatest* and *Second greatest* categories. Seven rules make up the rule-set used in the RET detection system. These are evaluated one after the other; however, once a given rule has been satisfied for the given road location, then the remaining rules are skipped. The rules serve the purpose of choosing between the 'competing' RET categories. The textual rules are given in [8].

IV. UNDERSTANDING THE COMPETITION HANDLING RULES VIA VISUALIZATION

In this section, the decision rules mentioned above are transcribed into a graphic representation to make them more understandable for a developer (e.g., of a road-related heuristic rule-based detection system for some other purpose). The resulting transcriptions (i.e., the graphic rule representations) look like graphical database queries [13].

A. Legend for the graphical representation

The cells of the table that are relevant for a given rule are coloured red, or green, while the categories appearing in these are printed in black (Figs. 2 - 8). E.g., SR *Kicker* is printed in black with a green background in Fig. 2, which represents Rule 1, while LR *Greatest,* also printed in black, is printed with a red background.

Each cell refers to the RET associated with the category indicated in respect of the given distance-scale (e.g., SR).

The green background within a cell indicates that the corresponding RET is to be chosen by that rule – if at all reached – as the RET perceived at the current road location of the ego-car.

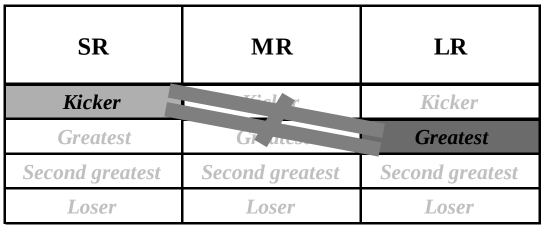

Figure 2. Graphic representation of Rule 1.

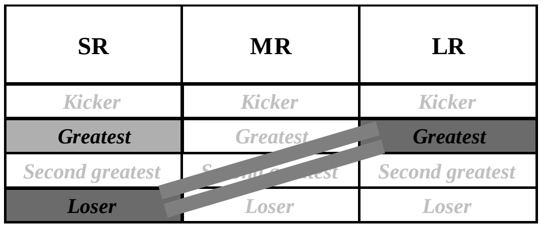

Figure 3. Graphic representation of Rule 2.

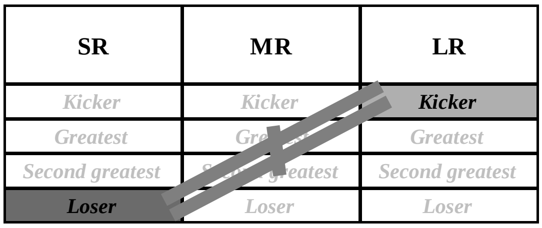

Figure 4. Graphic representation of Rule 3.

The red background indicates that the corresponding RET is rejected (i.e., the perceived RET differs from this one). The rotated '=' and '≠' signs express the required relation between the RETs associated with the corresponding cells.

Note that Rules 1 - 3 handle the case of a fast-changing road environment; these rules are presented graphically in Figs. 2 - 4; while Rules 4 - 7 handle constant, and slowly changing road environment. These rules are represented in Figs. 5 - 8.

V. DETECTION RESULTS

After experimenting with various score-calculations, and with various difference-thresholds for the *Kicker* and *Loser* category-assignments, an agreement in respect of the RETs of 66.5% was achieved for the test-route in Vác, Hungary. The length of this test-route was about 10 km.

This agreement is not impressive, but considering that only a small set of TSs was used for the purpose, this percentage is still reasonable. For details, see [8].

VI. CONCLUSIONS AND FUTURE WORK

A heuristic approach for RET detection around an ego-car was presented in [8]. The system described therein relies on TS data detected by an on-board TSR system. The collected TS data is stored in a FIFO queue, and repetitively processed in a multi-scale manner as explained in Subsect. III.A.

SR	MR	LR
Kicker	*Kicker*	***Kicker***
Greatest	***Greatest***	*Greatest*
Second greatest	*Second greatest*	*Second greatest*
Loser	*Loser*	*Loser*

(a)

SR	MR	LR
Kicker	*Kicker*	***Kicker***
Greatest	*Greatest*	*Greatest*
Second greatest	***Second greatest***	*Second greatest*
Loser	*Loser*	*Loser*

(b)

Figure 5. Graphic representation of Rule 4. The rule was brought up into two sub-rules; these are represented in separate tables (a) and (b).

SR	MR	LR
Kicker	*Kicker*	***Kicker***
Greatest	*Greatest*	*Greatest*
Second greatest	*Second greatest*	*Second greatest*
Loser	*Loser*	*Loser*

Figure 6. Graphic representation of Rule 5

SR	MR	LR
Kicker	*Kicker*	*Kicker*
Greatest	*Greatest*	***Greatest***
Second greatest	*Second greatest*	*Second greatest*
Loser	*Loser*	*Loser*

Figure 7. Graphic representation of Rule 6.

Last RET kept

Figure 8. Graphic representation of Rule 7.

From time to time, or perhaps more felicitously stated: from road-location to road-location, the choice between the RET-candidates selected for the different distance-scales is not evident, that is, a competition situation between the RET-candidates has appeared. The computation involved the candidate-selection is based on TS occurrences within the road-segments corresponding to the different distance-scales. To resolve the mentioned competition situation, the RETs are labeled – for each scale – with categories borrowed from the jargon used by sport competition juries. Then, the inter-range (i.e., overall, or final) decision on the actual RET perceived is made via the sequential evaluation of the proposed heuristic rules. In the present paper, these rules have been formulated in an intuitive, graphic (tabular) manner.

Assuming that a real-time TSR system is available on-board, and its detected TS data can be accessed for further processing (also in a real-time), then the management of the FIFO queue, and the evaluation of a few simple rules can be carried out also in a real-time manner (in respect of both the TSs and the RETs). This computation necessitates only low extra implementation costs.

The RET detection results achieved are compared in the cited paper to those acquired by an ANN-based implementation that relies solely on TS data. The main advantage of the rule-based approach is its readability and understandability, while heuristics amalgamates non-specific expert knowledge with commonsense. This advantage is further enhanced by the graphical representation employed herein. The proposed representation facilitates the reuse, the adaptation and the extension of the rule-set for other road-related applications that rely on TS, and possibly on other road-related data.

The agreement percentage for the RET detection approach would probably improve if a richer set of TS types were considered in the decision making process. On the other hand, the use of further road-related categories – supplementing the TS and CR categories already used in the cited papers – could facilitate the RET detection and improve its precision. Even the CR categories could be refined, and CRs could be extracted from a video-stream coming from an on-board camera, as described in [14].

We consider testing the RET detection methods – mentioned in the Introduction – on publicly available road-related datasets, e.g., on the Mapillary Vistas dataset (MVD) [15], as well. The MVD is large-scale street-level image dataset. It contains about 25 thousand high-resolution images annotated into 66 object-categories. The images in the dataset were taken at numerous urban locations from around the world in different weather conditions, in different seasons and at varied daytimes. Furthermore, the images come from different imaging devices (mobile phones, tablets, etc.), and were taken by photographers with different experience. Even if the direct use the mentioned dataset is uncertain in our case, as our methods rely on road-object (e.g., TS, CR) detections along contiguous trajectory-segments of the ego-car, the labels and categories used within the dataset provide expansion directions for improving and generalizing our methods.

Here, we list some of the more promising labels – particularly of static nature, i.e., excluding categories related to vehicles, people and animals – that are used in the annotations of the images: support: pole, utility-pole, TS-frame; object: street-light, billboard, traffic-light, fire-hydrant, bench, bike-rack, mailbox, phone-booth; TS: its front-side, its back-side; flat construction: road, sidewalk, curb-cut, parking area, bike-lane, service-lane, rail-track, pedestrian-area; barrier: curb, fence, wall, other barrier, guard-rail; structure: building, bridge, tunnel; road markings: general, crossroad-zebra. Location and category data on these street-level objects could provide further clues for RET inference.

The character of the road environment – even within the same socio-economic road environment – depends also on whether one is driving along a main road, or uses minor roads. This aspect of the RET detection was investigated in [12] using the fractal dimension of the trajectory, however, also the lane information from another ADAS subsystem could also be used for the purpose.

In order to achieve a RET detection precision necessary for automotive applications, an extensive international data collection effort would be imperative, as the urban textures of different geographical regions, cultures and countries differ significantly from one another.

References

[1] European Transport Safety Council, Briefing, “Intelligent speed assistance”, https://etsc.eu/briefing-intelligent-speed-assistance-isa, last accessed in March 2019.

[2] A. Møgelmose, M. M. Trivedi, and T. B. Moeslund,”Vision-based traffic sign detection and analysis for intelligent driver assistance systems: Perspectives and Survey,” *IEEE Trans. Intell. Transp*, vol. 13, pp. 1484–1497, 2012.

[3] Z. Fazekas, G. Balázs, L. Gerencsér, and P. Gáspár, “Inferring the actual urban road environment from traffic sign data using a minimum description length approach,” *Transp. Res. Proc*. vol. 27, pp. 516–523, 2017.

[4] R. Laguna, R. Barrientos, L. F. Blazquez, and L. J. Miguel. "Traffic sign recognition application based on image processing techniques," *IFAC Proceedings Volumes*, vol. 7, no. 3, pp. 104–109, 2014.

[5] Z. Fazekas, G. Balázs, L. Gerencsér, and P. Gáspár, “Detecting change in the urban road environment along a route based on traffic sign and crossroad data,” in *Intelligent Transport Systems – From Research and Development to the Market Uptake*, LNICST, Social Informatics & Telecommunications Engineering, vol. 222, Springer, 2018, pp. 252–262.

[6] Z. Fazekas, G. Balázs, and P. Gáspár, “ANN-based classification of urban road environments from traffic sign and crossroad data,” *Acta Polytech. Hung.* vol. 15, 2018, pp. 83–100.

[7] Z. Fazekas, G. Balázs, and P. Gáspár, “Building upon modularity in artificial neural networks,” *ERCIM News* vol. 116, pp. 30–31, 2019.

[8] Z. Fazekas, G. Balázs, and P. Gáspár, ”A heuristic approach to road environment-type detection from traffic sign data,” in Proc. of the 4th IEEE Conference on Control and Fault Tolerant Systems. Casablanca, Morocco, pp. 288–293, 2019.

[9] A. Venerandi, G. Quattrone, and L. Capra, “A scalable method to quantify the relationship between urban form and socio-economic indexes," *EPJ Data Sci.* vol. 7, pp. 1–21, 2018.

[10] A. Venerandi, G. Fusco, A. Tettamanzi, and D. Emsellem, D., “A machine learning approach to study the relationship between features of the urban environment and street value,” *Urban Science* vol. 3, issue 3, pp. 100–124, 2019.

[11] C. M. Rudin-Brown, J. Edquist, and M. G. Lenné, “Effects of driving experience and sensation-seeking on drivers’ adaptation to road environment complexity,” *Saf. Sci.* vol. 62, pp. 121–129, 2014.

[12] Z. Fazekas, G. Balázs, L. Gerencsér, and P. Gáspár, ”Experimenting with routes of different geometric complexity in the context of urban road environment detection from traffic sign data,” in *Integration as Solution for Advanced Smart Urban Transport Systems. TSTP 2018*, Advances in Intelligent Systems and Computing, vol 844, Springer, Cham, 2019. pp. 23–32.

[13] P. T. Wood. "Query languages for graph databases." *ACM Sigmod Rec.* vol. 41, pp. 50–60, 2012.

[14] C. Zhang, H. Fan, W. Li, B. Mao, and X. Ding, “Automated detecting and placing road objects from street-level images. *arXiv* preprint arXiv:1909.05621, 2019.

[15] G. Neuhold, T. Ollmann, S. Rota Bulò, and P. Kontschieder, “The Mapillary Vistas dataset for semantic understanding of street scenes,” in *Proceedings of the IEEE International Conference on Computer Vision*, pp. 4990–4999, 2017.